A nonlocal maximum likelihood estimation method for enhancing magnetic resonance phase maps

Sudeep, P. V.; Palanisamy, P.; Kesavadas, Chandrasekharan; Sijbers, Jan; Den Dekker, Arnold J.; Rajan, Jeny

DOI
10.1007/s11760-016-1039-6

Publication date
2017

Document Version
Accepted author manuscript

Published in
Signal, Image and Video Processing

Signal, Image and Video Processing (Accepted manuscript) manuscript No.
(will be inserted by the editor)

A Nonlocal Maximum Likelihood Estimation Method for Enhancing Magnetic Resonance Phase Maps

P V Sudeep · P Palanisamy · Chandrasekharan Kesavadas · Jan Sijbers · Arnold J. den Dekker · Jeny Rajan

Received: date / Accepted: date

Abstract A phase map can be obtained from the real and imaginary components of a complex valued magnetic resonance (MR) image. Many applications, such as MR phase velocity mapping and susceptibility mapping, make use of the information contained in the MR phase maps. Unfortunately, noise in the complex MR signal affects the measurement of parameters related to phase (e.g, the phase velocity). In this paper, we propose a nonlocal maximum likelihood (NLML) estimation method for enhancing phase maps. The proposed method estimates the true underlying phase map from a noisy MR phase map and it also works if the magnitude MR image and the noise standard deviation are not given. Experiments on both simulated and real data sets indicate that the proposed NLML method has a better performance in terms of qualitative and quantitative evaluations when compared to state-of-the-art methods.

Keywords Denoising · magnetic resonance image · maximum likelihood estimation · noise · phase map

PV Sudeep (corresponding author)
Department of Electronics and Communication Engineering, National Institute of Technology - Tiruchirappalli, Tamil Nadu, India
Department of Electronics and Communication Engineering, National Institute of Technology Karnataka, Surathkal, India
E-mail: spvnitt@gmail.com

P Palanisamy
Department of Electronics and Communication Engineering, National Institute of Technology - Tiruchirappalli, Tamil Nadu, India

Chandrasekharan Kesavadas
Department of Imaging Sciences and Intervention Radiology, Sree Chitra Tirunal Institute for Medical Sciences and Technology, Trivandrum, Kerala, India

Jan Sijbers
iMinds Vision Lab, Department of Physics, University of Antwerp, Belgium

Arnold J. den Dekker
iMinds Vision Lab, Department of Physics, University of Antwerp, Belgium
Delft Center for Systems and Control, Delft University of Technology, 2628 CD Delft, The Netherlands

Jeny Rajan
Department of Computer Science and Engineering, National Institute of Technology Karnataka, Surathkal, India

1 Introduction

The magnetic resonance (MR) magnitude and phase images are produced from the raw k-space data (after Fourier transform) acquired using the quadrature receivers of the magnetic resonance imaging (MRI) scanner. The magnitude image provides information on the structure and function of the soft tissue structures such as heart, liver, brain and other organs. The phase images (or phase maps), on the other hand, provide information such as field inhomogeneity or velocity of blood flow and this information is used in many MR applications such as phase contrast angiography, blood oxygenation level dependent (BOLD) MR venography, the computation of field maps for the geometric correction of echo planar images, or MR thermometry [21]. Susceptibility weighted imaging (SWI) also relies on phase and magnitude MR data to visualize venous structures and iron content in the brain [22]. Unfortunately, both magnitude and phase images are corrupted with noise, which is mainly thermal in origin.

The noise present in the k-space data can substantially deteriorate the quality and brings down the overall SNR of the phase map [5]. Denoising is one way to improve the SNR of MR phase images. Nevertheless,

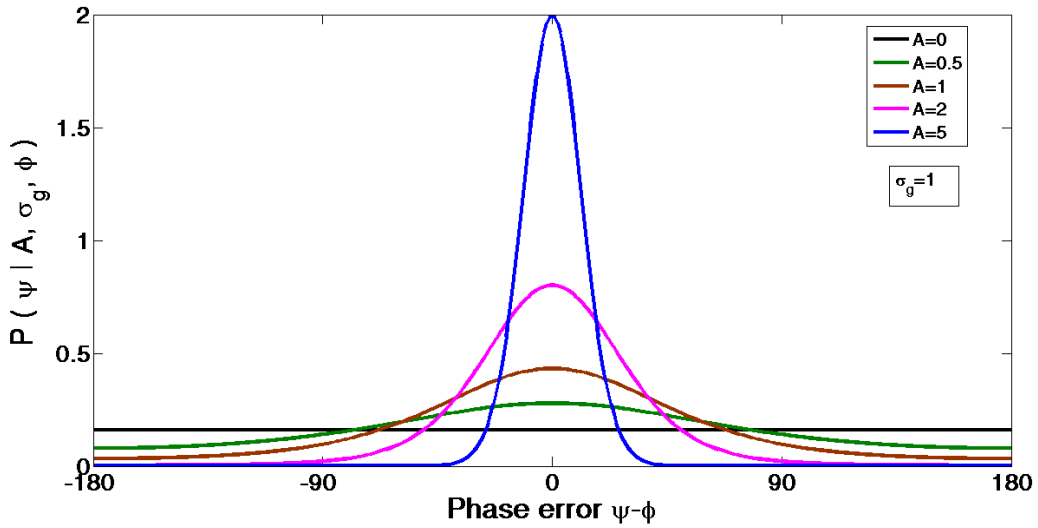

Fig. 1 Distribution of phase as a function of phase error for several values of A and $\sigma_g = 1$.

only a few approaches have been proposed in the literature to denoise MR phase maps.

Lorenzo-Ginori *et al.* [13] proposed a nonlinear vector filter to reduce the noise in the phase map. This nonlinear vector filter, which uses similarity measures based on angular distances, was adapted to phasor processing and used to filter the complex image from which the phase is obtained. Cruz-Enriquez *et al.* [6] extended this work by combining the nonlinear filter with wavelet techniques. They decomposed the real and imaginary components of the noisy complex signal using the Discrete Wavelet Transform (DWT) and the nonlinear vector is applied to each part, and finally, the filtered image is recovered by inverse DWT-2D transformation. However, the aforementioned methods require both observed magnitude and phase data to denoise the phase map and will not be useful when only the noisy phase map is available. The adaptive local denoising method (also referred to as PEARLS) in [2] is another phase estimation method proposed in the literature based on local polynomial approximations. This method was originally introduced for synthetic aperture radar (SAR) images.

Many methods have been proposed in the literature to denoise MR magnitude images (e.g.,[1, 15, 24, 10, 23, 9, 17, 19, 20, 14, 12]). Among them, the NLML methods proposed recently in the literature for denoising MR magnitude images are promising and that motivated us to extend the NLML method to denoise MR phase images in this paper. One advantage of the proposed phase NLML (P-NLML) method is its ability to denoise phase maps even if magnitude images are not available. (e.g., in certain flow imaging studies like cerebrospinal fluid and blood flow studies, the information from phase images alone is used and in such cases magnitude images may not be stored.) The rest of the paper is organized as follows: the relevant background on the noise in MR phase maps and the ML estimation theory are provided in section 2. Section 3 explains the proposed approach for noise removal in MR phase maps. Experimental results are reported in Section 4 and the paper is concluded in Section 5.

2 Theory

The acquired MR data are generally corrupted with noise. The noise in the real and imaginary components of the complex MR signal are assumed to be independent and identically distributed (i.i.d.) zero mean Gaussian with equal variance σ_g^2. Let A and ϕ be the true amplitude and the true phase in a given pixel, respectively. After the polar transform, the calculated magnitude M and the phase ψ are given by [3, 7]:

$$M = \sqrt{(A\cos\phi + n_{re})^2 + (A\sin\phi + n_{im})^2} \quad (1)$$

$$\psi = \arctan\left(\frac{A\sin\phi + n_{im}}{A\cos\phi + n_{re}}\right) \quad (2)$$

where n_{re} and n_{im} are the noise components in the real and imaginary images respectively.

The joint density of M and ψ can be expressed as [3, 7]:

$$P(M,\psi|A,\sigma_g,\phi) = \frac{M}{2\pi\sigma_g^2} e^{-\frac{1}{2\sigma_g^2}\left[M^2+A^2-2AM\cos(\psi-\phi)\right]} \quad (3)$$

The integration of Eq. (3) over M yields the marginal probability density of the MR phase data and is given by [7]:

$$P(\psi|A,\sigma_g,\phi) = \frac{1}{2\pi} e^{\frac{-A^2}{2\sigma_g^2}} \left[1 + \kappa\sqrt{\pi} e^{\kappa^2} \left(1 + \mathrm{erf}(\kappa)\right)\right] \tag{4}$$

where

$$\kappa = \frac{1}{\sqrt{2}} \frac{A}{\sigma_g} \cos\left(\psi - \phi\right) \tag{5}$$

The phase probability density function (PDF) $P\left(\psi|A,\sigma_g,\phi\right)$ is plotted as a function of phase error at different SNRs, defined as the ratio A/σ_g, in Fig. 1. The phase error represents the deviation of the noisy phase ψ from its true value ϕ. This figure demonstrates that the phase PDF at low SNR is uniform and rapidly converges towards a Gaussian distribution as SNR increases.

3 Methods

3.1 The non-local maximum likelihood method for phase estimation (P-NLML1)

Nonlocal (NL) versions of the ML estimation method have been proposed in the literature for the enhancement of Rician distributed magnitude MR images [9, 17, 19, 20]. Motivated by those approaches, a new NLML estimation method for enhancing MR phase maps described by Eq. (4) is proposed in this paper. The nonlocal principle exploits the redundancy of patches in an image. Here the assumption is that, if two neighborhoods are similar, then their center pixels should have similar phase values. They can be considered as two noisy measurements of the same noise-free pixel.

Let $\boldsymbol{\psi} = [\psi_1, \psi_2, \cdots, \psi_N]$ be N statistically independent observations from a region of constant phase ϕ. Assume that σ_g be the standard deviation of the noise and $\boldsymbol{A} = [A_1, A_2, \cdots, A_N]$ be the corresponding true magnitude intensity values. Then, the ML estimator of ϕ can be derived from the marginal density given by Eq. (4).

The ML estimate of ϕ can be computed by maximizing the likelihood function $\mathcal{L}(\boldsymbol{\psi}|\boldsymbol{A},\sigma_g,\phi)$ or equivalently by maximizing the log-likelihood function $\log\mathcal{L}(\boldsymbol{\psi}|\boldsymbol{A},\sigma_g,\phi)$ with respect to ϕ , which is given below :

$$\begin{aligned}\log\mathcal{L}(\boldsymbol{\psi}|\boldsymbol{A},\sigma_g,\phi) &= \sum_{j=1}^{N} \log P(\psi_j|A_j,\sigma_g,\phi) \\ &= -N\log 2\pi - \frac{\sum_{j=1}^{N} A_j^2}{2\sigma_g^2} \\ &+ \sum_{j=1}^{N} \log[1 + \kappa_j\sqrt{\kappa_j^2}(1 + \mathrm{erf}\left(\kappa_j\right))].\end{aligned} \tag{6}$$

Furthermore, the ML estimator of the unknown true phase ϕ is given by,

$$\hat{\phi}_{ML} = \arg\max_{\phi} \left(\log\mathcal{L}(\boldsymbol{\psi}|\boldsymbol{A},\sigma_g,\phi)\right). \tag{7}$$

The ML estimator described by Eq. (7) requires the noiseless or denoised magnitude values of $\boldsymbol{A}$. The magnitude MR data in the presence of noise follows a Rician distribution and the PDF is given by [25]:

$$p\left(M|A,\sigma_g\right) = \frac{M}{\sigma_g^2} e^{-\frac{\left(M^2+A^2\right)}{2\sigma_g^2}} I_0\left(\frac{AM}{\sigma_g^2}\right) H\left(M\right), \tag{8}$$

where I_0 is the zeroth order modified Bessel function of the first kind. Here, M denotes the Rician distributed random variable, A is the noise free MR signal and $H\left(\cdot\right)$ represents the Heaviside step function. The shape of the Rice PDF also depends on the SNR. At high SNR, i.e. when $A/\sigma_g \to \infty$, the Rician distribution approaches a Gaussian distribution and when the SNR is zero (e.g, in the background), the data will follow a Rayleigh distribution. In our experiments, we computed the denoised magnitude values of $\boldsymbol{A}$ with the method described in [19].

When both magnitude and phase data are available, we used Eq. (7) to implement the P-NLML1 filter as explained in Algorithm 1. In the proposed method, we measured the similarity using the Euclidean distance $d_{x,y}$ between the phase value vector θ of neighborhoods B_x and B_y around the locations (i.e., pixels) x and y (excluding the phase values at x, y), respectively. It is defined as [9, 20]:

$$d_{x,y} = \|\theta(B_x) - \theta(B_y)\| \tag{9}$$

For each phase location x in the phase map, the intensity distance $d_{x,y}$ between x and all other nonlocal locations y, as defined by Eq. (9), in the *search window* are measured. After sorting the non local pixels (observed phase values) in the increasing order of $d_{x,y}$, the first k pixels are selected for ML estimation. In our implementation we fix k to 25 as recommended in [9].

With P-NLML1, we have to estimate the noise standard deviation σ_g and we estimated this parameter from the magnitude image prior to applying Eq. (7). In

Algorithm 1 P-NLML1 Filter for single parameter estimation

Input: $\boldsymbol{\Theta} \Leftarrow$ Noisy MR phase data
$\sigma_g \Leftarrow$ noise standard deviation
$\mathbf{A} \Leftarrow$ Magnitude data
for each pixel $\theta(x)$ of $\boldsymbol{\Theta}$ **do**
  Select a $T \times T$ *Search Window* around the pixel
  $B_x \Leftarrow$ *Similarity window* of size $t \times t$ around the pixel
  $B_y \Leftarrow$ Non local neighbourhood windows in the *Search Window* other than B_x
  Compute the distance $\|\theta(B_x) - \theta(B_y)\|$ and create a list d
  $D = sort(d)$ i.e., rank d in ascending order.
  Choose the first k elements of D.
  Compute $\hat{\phi}_{ML} \leftarrow$ ML estimation of the samples using Eq. (7).
end for
Output: $\hat{\boldsymbol{\Phi}} \Leftarrow$ Denoised MR phase data

Algorithm 2 P-NLML2 Filter for three parameter estimation

Input: $\boldsymbol{\Theta} \Leftarrow$ Noisy MR phase data
for each pixel $\theta(x)$ of $\boldsymbol{\Theta}$ **do**
  Select a $T \times T$ *Search Window* around the pixel
  $B_x \Leftarrow$ *Similarity window* of size $t \times t$ around the pixel
  $B_y \Leftarrow$ Non local neighbourhood windows in the *Search Window* other than B_x
  Compute the distance $\|\theta(B_x) - \theta(B_y)\|$ and create a list d
  $D = sort(d)$ i.e., rank d in ascending order.
  Choose the first k elements of D.
  Compute $\hat{\phi}_{ML}, \hat{A}_{ML}, \hat{\sigma_g}_{ML} \leftarrow$ ML estimation of the samples using Eq. (10).
end for
Output: $\hat{\boldsymbol{\Phi}} \Leftarrow$ Denoised MR phase data
$\boldsymbol{\sigma}_g \Leftarrow$ Matrix of standard deviations
$\mathbf{A} \Leftarrow$ Estimate of magnitude data

the past, many robust methods have been proposed in the literature for the estimation of the noise level from a single magnitude MR image and a survey of these methods is given by Aja-Fernández *et al.*[1]. In this paper, we followed the ML based method proposed in [16] for the estimation of σ_g to work with the P-NLML1 filter.

3.2 P-NLML method for three parameter estimation (P-NLML2)

Even though the ML scheme for single parameter estimation ($\hat{\phi}_{ML}$) in Eq. (7) is useful to estimate the true underlying phase value, this approach fails in situations when both $\boldsymbol{A}$ and σ_g are not provided. In that case we estimated all the three unknown parameters by maximizing the likelihood function $\mathcal{L}$ or equivalently $\log \mathcal{L}$, with respect to A, σ_g and ϕ as given below:

$$\left\{\hat{\phi}_{ML}, \hat{A}_{ML}, \hat{\sigma_g}_{ML}\right\} = \arg \max_{\phi, A, \sigma_g} \left(\log \mathcal{L}(\boldsymbol{\psi}|A, \sigma_g, \phi)\right). \tag{10}$$

We referred the P-NLML filter for three parameter estimation, which uses Eq. (10) in the presence of phase data alone, as P-NLML2 filter. In Eq. (10), we conveniently assumed that the values of A, σ_g and ϕ are constant for all the k selected nonlocal pixels. The validity of this assumption may be questioned, since pixels that have similar phase values do not necessarily have the same magnitude values. Nevertheless, the experimental results show that the results of P-NLML2 are comparable with P-NLML1.

The aforementioned ML scheme for three parameter estimation can be considered as a multidimensional unconstrained nonlinear maximization problem and the ML estimates of the parameters can be found numerically using nonlinear optimization algorithms.

4 Experiments and Results

4.1 Visual quality comparison with simulated phasemap

For simulations, we used the data set given in [11] (data sets are from the 2010 ISMRM Recon Challenge). The Ground Truth (GT) (complex data) is corrupted with Gaussian noise to create the noisy phase maps. For a comparative analysis, we also did experiments with two different versions of the nonlocal means (NLM) [4] method (denoted as NLM1 and NLM2 respectively) and the local ML filter. The NLM1 filter is the conventional NLM filter directly applied to the phase maps.

Table 1 Technical details of different denoising methods

Method	Input	Output	Filter Parameters
NLM1	ψ and σ_g only	$\hat{\phi}$	search window size = 11×11, similarity window size = 3×3
NLM2	A and ψ; or, complex data	$\hat{\phi}$	
P-LML		$\hat{\phi}$	window size= 3×3
P-NLML2	ψ only	$\hat{\phi}$,$\hat{A}$,$\hat{\sigma_g}$	search window size = 11×11, similarity window size = 3×3 and sample size k = 25
P-NLML1	A and ψ; or, complex data	$\hat{\phi}$	

Table 2 Comparison of experimental results based on PSNR

Method	PSNR							
	$\sigma = 5$	$\sigma = 10$	$\sigma = 15$	$\sigma = 20$	$\sigma = 25$	$\sigma = 30$	$\sigma = 35$	$\sigma = 40$
Noisy	5.7049	3.8857	3.0921	2.6916	2.4411	2.2317	2.0633	1.9341
NLM1	11.0101	8.4138	7.1003	6.3709	5.9316	5.5494	5.2677	5.0437
NLM2	9.9339	8.4790	7.3319	6.6582	5.9997	5.5850	4.9709	4.8572
P-LML	10.0642	7.1830	5.6215	4.8211	4.3160	4.0989	3.8531	3.6406
P-NLML2	11.6206	8.8789	7.1714	6.6230	6.0254	5.6733	5.3308	**5.3163**
P-NLML1	**12.7820**	**10.0891**	**8.3250**	**7.4086**	**6.7117**	**6.0395**	**5.5005**	5.3056

The NLM2 filter works on the complex data to achieve an enhanced phase map.

The denoising methods were carried out with the following parameters: (i) NLM1 and NLM2 filters: search window size = 11×11 similarity window size = 3×3. The noise variance σ_g^2 used in both methods was estimated using the local ML method mentioned in [16]. (ii) local ML method for single parameter estimation (P-LML): window size= 3×3 (iv) proposed P-NLML1 and P-NLML2 filters : search window size = 11×11, neighborhood size = 3×3 and sample size $k = 25$. The input and output variables as well as the filter parameters of all methods considered are summarized in Table 1.

For the experimental results shown in Fig. 2, we corrupted the Ground Truth (complex image) with Gaussian noise of $\sigma_g = 15$. It can be observed from the results that the noisy phase map denoised with the proposed P-NLML1 filter is much closer to the original phase map than the phase map produced by the NLM1 Filter, the NLM2 filter and the P-LML method. Even though the performance of the P-NLML2 filter is inferior to the P-NLML1 filter due to the simultaneous estimation of three parameters which reduces the precision of ML estimation, it does improve the quality of the phase map. Qualitatively, the proposed P-NLML filters provide fewer oscillations over homogeneous areas and better noise removal than the other methods under consideration. For quantitative analysis, the GT was degraded with Gaussian noise for a wide range of noise levels (σ_g varying from 5 to 40) and the corresponding phase maps are created. The denoising efficiency of NLM1, NLM2, P-LML, P-NLML1 and P-NLML2 were evaluated based on the Peak Signal to Noise Ratio (PSNR) [8]. The PSNR is the simplest and most widely used quality measure for 2D signals evaluated in decibels (dB) which is given by:

$$\text{PSNR} = 20\log_{10}\frac{\text{MAX}}{\text{RMSE}}, \tag{11}$$

where MAX is the maximum intensity value in the original phase map and RMSE denotes the root mean square error estimated between the ground truth and the denoised phase map. In Table 2, we can observe that the P-NLML methods outperform over other filters in terms of the objective measure PSNR.

4.2 Visual quality comparison with real phasemap

In order to validate the performance of the proposed method on real data, we conducted experiments on kiwi fruit phase maps of size 256×256 acquired with a 9T MR scanner using a slice thickness of 0.4 mm. Our proposed methods provide better results in terms of noise removal than other aforementioned filters when the same noisy MR phase maps are provided as input (see Fig. 3). For P-NLML1, the noise standard deviation was estimated from the corresponding magnitude image and the unknown true underlying intensity A was estimated using the conventional NLML method. In this experiment the sample size k was fixed as 25 for both P-NLML1 and P-NLML2.

We also carried out an experiment on a single 2D phase image reconstructed from a fully sampled single coil MR image. This MR angiography image was

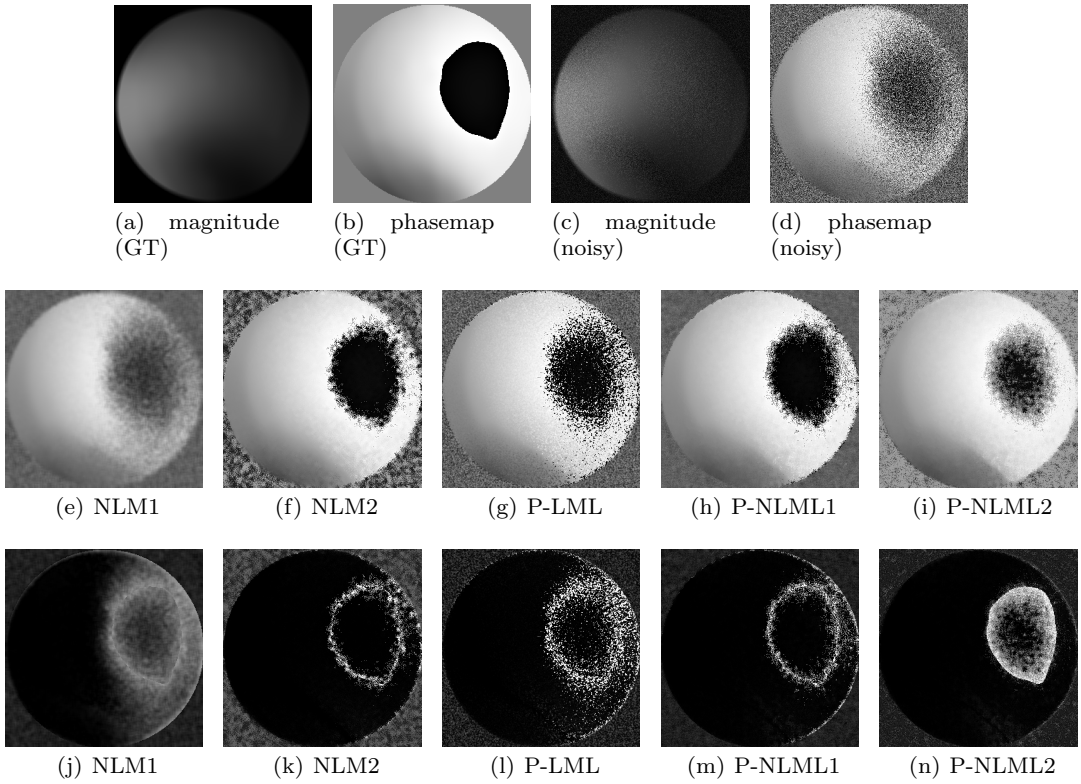

(a) magnitude (GT) (b) phasemap (GT) (c) magnitude (noisy) (d) phasemap (noisy)

(e) NLM1 (f) NLM2 (g) P-LML (h) P-NLML1 (i) P-NLML2

(j) NLM1 (k) NLM2 (l) P-LML (m) P-NLML1 (n) P-NLML2

Fig. 2 Denoising of simulated phase map with various methods (a) Original simulated magnitude image (b) Original simulated phase map (c) Noisy magnitude image ($\sigma_g = 15$) (d) Noisy phase map ($\sigma_g = 15$) (e) Denoised phase map using the NLM1 filter (f) Denoised phase map using the NLM2 filter (g) Denoised phase map using P-LML filter for single parameter estimation (h) Denoised phase map using the P-NLML1 filter (i) Denoised phase map using the P-NLML2 filter and (j)-(n) the residuals of images in (e)- (i) respectively. (residuals in the range $0 - 2\pi$).

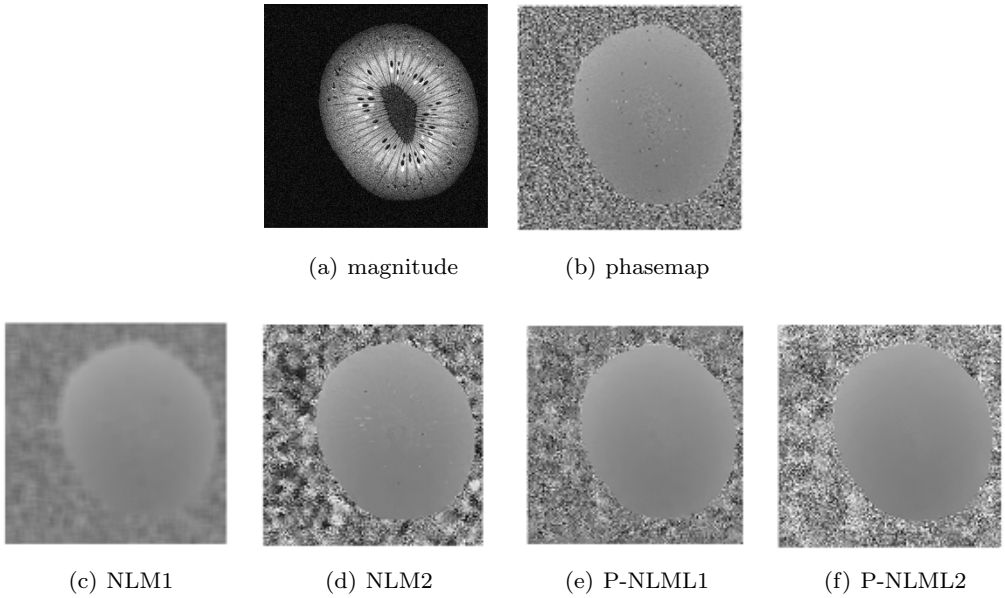

(a) magnitude (b) phasemap

(c) NLM1 (d) NLM2 (e) P-NLML1 (f) P-NLML2

Fig. 3 Denoising of real kiwi fruit MR phase map with various methods (a) Noisy kiwi fruit magnitude image (b) Noisy kiwi fruit phase map (c) Denoised phase map using the NLM1 filter (d) Denoised phase map using the NLM2 filter (e) Denoised phase map using the P-NLML1 filter (f) Denoised phase map using the P-NLML2 filter.

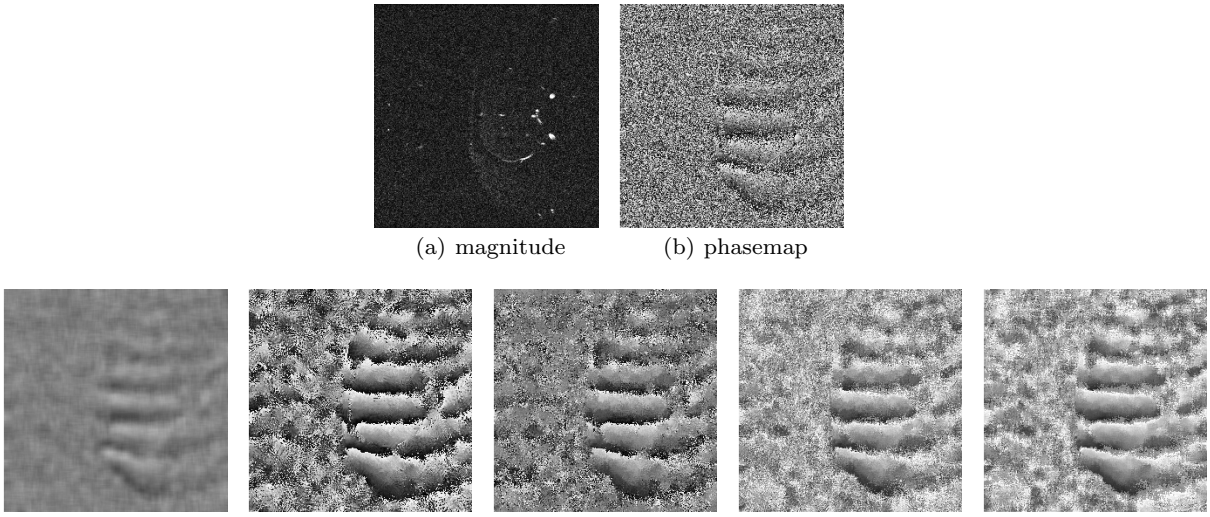

(a) magnitude (b) phasemap

(c) NLM1 (d) NLM2 (e) P-NLML1 (f) P-NLML2 (#samples=25) (g) P-NLML2 (#samples=55)

Fig. 4 Denoising of real brain MR phase map with various methods (a) Noisy magnitude image (b) phase map (c) Denoised phase map using the NLM1 filter (d) Denoised phase map using the NLM2 filter (e) Denoised phase map using the P-NLML1 filter with 25 samples for ML estimation (f) Denoised phase map using the P-NLML2 filter with 25 samples for ML estimation (g) Denoised phase map using the P-NLML2 filter with 55 samples for ML estimation.

acquired with the following parameters: matrix size of 256×256, number of slices 120, both fat and flow saturation "on". In Fig. 4 (e) and Fig. 4 (f), we compared the denoising results of P-NLML1 and P-NLML2 filters by fixing the number of samples for ML estimation to 25. Fig. 4 (g) shows the result of P-NLML2 with sample size 55. When we compare Fig. 4 (f) and Fig. 4 (g), it can be noticed that in homogeneous regions Fig. 4 (g) is superior to Fig. 4 (f). However over smoothing can be observed along the edges in Fig. 4 (g). The results of other filters such as NLM1 and NLM2 are also displayed. It can be observed from Fig. 4 that the results obtained with P-NLML2 are comparable with those obtained with the methods that require magnitude data for denoising the phase map. The performance of the proposed NLML methods can be significantly improved by adaptively selecting the number of samples k (for each and every pixel) for the ML estimation. A too low or high value of k can cause under or over smoothing [18].

5 Conclusion

In this paper, we present NLML filters to reduce noise in MR phase data. These nonlocal maximum likelihood filters achieved significant enhancement in the phase map both visually as well as quantitatively (in terms of PSNR). The performance of these filters has been analyzed
through experiments conducted on both simulated and real phase maps. The performance of the proposed method can further improve through adaptive selection of sample sizes for ML estimation. Further research is required in this direction.

References

1. Aja-Fernández S, Alberola-López C, Westin C (2008) Noise and signal estimation in magnitude MRI and Rician distributed images:a LMMSE approach. IEEE Trans Imag Proc 17:1383–1398
2. Bioucas-Dias J, Katkovnik V, Astola J, Egiazarian K (2002) Absolute phase estimation: adaptive local denoising and global unwrapping. Applied Optics 47(29):5358–5369
3. Bonny JM, Renou JP, Zanca M (1996) Optimal measurement of magnitude and phase from MR data. Journal of Magnetic Resonance, Series B 113(2):136 – 144
4. Buades A, Coll B, Morel JM (2005) A review of image denoising algorithms, with a new one. Multiscale Model Simul 4:490–530
5. Chavez S, Xiang QS, An L (2002) Understanding phase maps in MRI: a new cutline phase unwrapping method. IEEE Trans Med Imag 21(8):966–977
6. Cruz-Enrquez H, Lorenzo-Ginori J (2009) Combined wavelet and nonlinear filtering for MRI phase images. In: Kamel M, Campilho A (eds) Image Analysis and Recognition, Lecture Notes in Com-

puter Science, vol 5627, Springer Berlin Heidelberg, pp 83–92, iSBN: 978-3-642-02610-2
7. den Dekker AJ, Sijbers J (2014) Data distributions in magnetic resonance images: A review. Physica Medica 30(7):725–741
8. Fisher Y (1995) Pixelized Data. Springer-Verlag London
9. He L, Greenshields IR (2009) A nonlocal maximum likelihood estimation method for Rician noise reduction in MR images. IEEE Trans Med Imaging 28:165–172
10. Heydari M, Karami MR, Babakhani A (2016) A new adaptive coupled diffusion PDE for MRI Rician noise. Signal, Image and Video Processing pp 1–8
11. ISMRM (2010) `http://www.ismrm.org/mri_unbound/simulated.htm`
12. Krissian K, Aja-Fernández S (2009) Noise-driven anisotropic diffusion filtering of mri. IEEE transactions on image processing 18(10):2265–2274
13. Lorenzo-Ginori JV, Plataniotis KN, Venetsanopoulos AN (2002) Nonlinear filtering for phase image denoising. IEEE Proc on Vision, Image and Signal Processing 149(5):290–296
14. Manjón JV, Carbonell-Caballero J, Lull JJ, García-Martí G, Martí-Bonmatí L, Robles M (2008) Mri denoising using non-local means. Medical image analysis 12(4):514–523
15. Mohan J, Krishnaveni V, Guo Y (2014) A survey on the magnetic resonance image denoising methods. Biomedical Signal Processing and Control 9:56 – 69
16. Rajan J, Poot D, Juntu J, Sijbers J (2010) Noise measurement from magnitude MRI using local estimates of variance and skewness. Phys Med Biol 55:N441–N449
17. Rajan J, Jeurissen B, Verhoye M, Van Audekerke J, Sijbers J (2011) Maximum likelihood estimation-based denoising of magnetic resonance images using restricted local neighborhoods. Phys Med Biol 56:5221–5234
18. Rajan J, Van Audekerke J, Van der Linden A, Verhoye M, Sijbers J (2012) An adaptive non local maximum likelihood estimation method for denoising magnetic resonance images. In: 2012 9th IEEE International Symposium on Biomedical Imaging (ISBI), IEEE, pp 1136–1139
19. Rajan J, Veraart J, Van Audekerke J, Verhoye M, Sijbers J (2012) Nonlocal maximum likelihood estimation method for denoising multiple coil magnetic resonance images. Magn Reson Imaging 30(10):1512–1518
20. Rajan J, den Dekker AJ, Sijbers J (2014) A new non-local maximum likelihood estimation method for Rician noise reduction in magnetic resonance images using the Kolmogorov-Smirnov test. Sign Proc 103(0):16–23
21. Rauscher A, Barth M, Reichenbach JR, Stollberger R, Moser E (2003) Automated unwrapping of MR phase images applied to BOLD MR venography at 3 Tesla. Magn Reson Imaging 18(2):175–180
22. Rauscher A, Barth M, Reichenbach JR, Stollberger R, Moser E (2005) Magnetic susceptibility-weighted MR phase imaging of the human brain. Journ Neuro Radiol 26(4):736–742
23. Riji R, Rajan J, Sijbers J, Nair MS (2015) Iterative bilateral filter for Rician noise reduction in MR images. Signal, Image and Video Processing 9(7):1543–1548
24. Sharif M, Hussain A, Jaffar MA, Choi TS (2016) Fuzzy-based hybrid filter for Rician noise removal. Signal, Image and Video Processing 10(2):215–224
25. Sijbers J, den Dekker AJ, Scheunders P, Van Dyck D (1998) Maximum likelihood estimation of Rician distribution parameters. IEEE Trans Med Imag 17(3):357–361